FFI-RAPPORT

16/01542

Beamforming of synthetic target signal acquired by the Atlantis PCL system

–

Kyrre Strøm[1]
Erlend Finden[1]
Jochen Schell[2]
Idar Norheim-Næss[1]
Øystein Lie-Svendsen[1]

[1] Norwegian Defence Research Establishment
[2] Fraunhofer FHR

Beamforming of synthetic target signal acquired by the Atlantis PCL system

Kyrre Strøm[1]
Erlend Finden
Jochen Schell[2]
Idar Norheim-Næss[1]
Øystein Lie-Svendsen[1]

[1] Norwegian Defence Research Establishment [2] Fraunhofer FHR

Norwegian Defence Research Establishment (FFI) 20 September 2016

Keywords

Radar
Signalbehandling
Antenne

FFI-RAPPORT:
2016/01542

Project number:
129701

ISBN:
P: 978-82-464-2796-6
E: 978-82-464-2797-3

Approved by:
Johnny Bardal, *Director*
Karl Erik Olsen, *Research Manager*

Summary

The passive coherent location system, Atlantis, is a test bed for digital beamforming at the Norwegian Defence Research Establishment (FFI). The system has functionality for real time direction of arrival (DoA) estimation. An acquisition experiment involving a synthetic target has been conducted for the purpose of investigating the DoA estimation capabilities of polarized signals. Data recorded during the experiment was subsequently processed offline to test the effect of various beam patterns. The offline processing underlying this report made use of Matlab -scripts replacing the beamscan algorithms of Atlantis. Some findings from this experiment are that DoA estimation works fine for target signals that are co-polarized with the receiver antenna, and for signals where the co-polarized component makes a substantial part of the signal. On the other hand, target signals that are mainly cross-polarized with the receiver antenna appear with a diffuse and sometimes incorrect location. In addition to DoA estimations, attempts were made of suppressing an unwanted signal by placing one or more static nulls in the direction of the known synthetic target signal. Suppression attempts were made for target signals that were co-polarized with the receiver antenna as well as for cross-polarized signals. In the co-polarized case a substantial reduction of the signal noise ratio (SNR) at the nulled signal direction occurred when that direction appeared within 20° from the mainlobe direction. When the synthetic target direction appeared further from the mainlobe, placing a null in the target direction had little effect. Even though the reduction close to the mainlobe was substantial for a single null, it was in most cases more profound when three close nulls were placed in the direction of the synthetic target. Nulling a signal cross-polarized with the receiver antenna turned out problematic.

Sammendrag

Den passive bistatiske radaren, Atlantis, er et testsystem for digital stråleforming ved Forsvarets Forskningsinstitutt (FFI). Systemet har funksjonalitet for sanntids retningsbestemmelse av innkommende signal. Et eksperiment for opptak av signaler fra et syntetisk mål er utført. Hensikten med eksperimentet var å undersøke egenskapene for retningsbestemmelse av polariserte signaler. Data innsamlet under eksperimentet ble i ettertid prosessert off-line for å undersøke effekten av ulike strålingsmønstre. Offline-processeringen som ligger til grunn for denne rapporten, benyttet Matlab-skript som erstattet beamscan-algoritmene i Atlantis. Noen funn fra dette eksperimentet er at retningsbestemmelse virker godt for målsignal som er ko-polarisert med mottagerantennen, og for signaler hvor den ko-polariserte komponenten utgjør en vesentlig del av signalet. Målsignaler som hovedsakelig er kryss-polarisert med mottagerantennen fremkommer med diffus og noen ganger uriktig retningsangivelse. I tillegg til retningsbestemmelse er det gjort forsøk på å undertrykke uønsket signal ved å plassere en eller flere statiske nuller i den kjente retningen for det syntetiske målet. Forsøket på undertrykking ble gjort for signaler som var kryss-polarisert med mottagerantennen så vel som for ko-polariserte signaler. I det ko-polariserte tilfellet oppnådde vi en vesentlig reduksjon i signal til støy-forholdet (SNR) for den nullede mål-signal retningen så lenge den retningen var mindre enn 20grader fra hovedloberetningen. Når retningen for det syntetiske målet var lenger fra hovedloben, hadde det liten virkning å plassere en null i den retningen. Selv om reduksjonen nær hovedloben var betydelig for en enkelt null, var den i de fleste tilfellene enda sterkere når tre tettsittende nuller ble plassert i retningen av det syntetiske målet. Nulling av signal som var kryss-polarisert med antennen, viste seg problematisk.

Contents

1 Introduction

Sensor arrays make it possible to apply spatial filtering techniques during signal processing of wavefields. Spatial filtering techniques, also denoted beamforming, is used for directional transmission as well as reception of signals. Array processing with both spatial and temporal filtering of received wavefield offers improved possibilites for enhancing the signal to noise ratio and characterisation of the wavefield. Compared to a single sensor an array sensor also offers a bigger toolbox for tracking signal sources, [3]. There is a wide range of array antennas that can perform various degree of beamforming. See e.g [8] for an introductory overview. A Passive Electronically Scanned Array (PESA) applies for all the antenna elements phase shifters to modify an electromagnetic wave centrally generated. Phase shifters make it possible to electronically change the pointing direction of the beam within milliseconds. An Active Electronically Scanned Array (AESA) has transmitter/receiver modules individual for each array element or for sub-groups of array elements. This offers greater flexibility to modify frequency of transmitted signal as well as both phase and amplitude of the signal for each array element. Beam patterns can be changed continuously, and sub-beams of various frequencies can be produced simultaneously making it possible to track a larger number of targets. A step even further is achieved by the Digitally Electronic Scanned Array (DESA). In these arrays there is an AD-converter for each array element or for groups of array elements. The digitized signal is processed by a computer that performs the beamforming digitally. The computer may form and process many reception beams simultaneously. How many is to a large extent governed by the computational power. The computer then presents to the radar operator the result from the beam that best fulfills a given criterion.

1.1 Planar waves beamforming

A radar with beamforming capabilities has an antenna consisting of several elements. The differences in geometric location of the antenna elements equip the radar with a filter that depends on the direction of the signal, but is independent of time. In receive mode, such a filter can enhance signals arriving from some directions while weakens or suppresses completely signals arriving from other directions. New spatial filters can be made by individually shifting the phase and scaling the amplitude of the signals received by each of the antenna elements before summing the result. These spatial filters depend on the frequency of the signal in addition to the direction of arrival. Such a linear filter is achieved by letting the phase shifts and amplitude scalings be defined by a set of weights associated with the antenna elements, one weight for each element. Various sets of weights define various beam patterns. For an antenna in receive mode the beam pattern is the output intensity from the spatial filter as a function of the arrival angle from boresight of an incoming plane wave. The incoming wave is then considered monochromatic and of unit amplitude.

To describe the spatial filtering in some more detail we follow [6] chapter 2. Let the incoming signal $s(t)$ be a monochromatic plane wave arriving from direction $\mathbf{r}$, and let $\mathbf{r_m}$ be the location of the m-th array element relative to a reference point O. $\mathbf{r}$ is the unit vector pointing from the reference point towards the signal source. The time delay for a wave front to reach from the reference point to the location of the m-th array element is $\tau_m = -\langle \mathbf{r}, \mathbf{r_m} \rangle / c$, where c is the signal velocity. So if $s_O(t) = s(t)$ is the signal reaching the reference point at time t, the signal reaching element m at

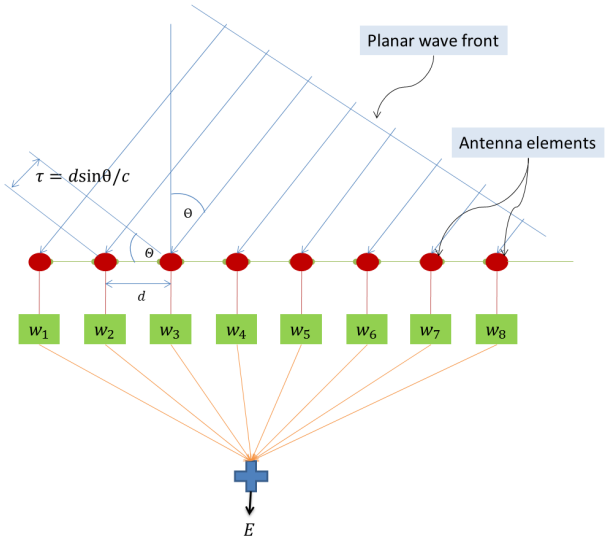

Figure 1.1 *Schematic drawing of linear array with planar wave arriving an angle θ from boresight.*

time t will be $s(t-\tau_m)$. Assuming the signal s is in complex analytic form we can offset the phase and scale the amplitude of the signal output from element m simply by multiplying with a complex number w_m. Summing the result we obtain a filtered output from the array antenna,

$$E(t) = \sum_m w_m s_m(t) \quad \text{where } s_m(t) = s(t-\tau_m)\,,\ \tau_m = -\langle \mathbf{r}, \mathbf{r_m} \rangle / c$$

For a narrowband signal with center frequency ν and wavelength $\lambda = c/\nu$ the time delay τ_m amounts to a phase shift $2\pi\nu\tau_m$. Indeed, for a monochromatic signal $s(t) = e^{2\pi i(\nu t+\psi_0)}$ we have $s(t-\tau_m) = e^{2\pi i(\nu t+\langle \mathbf{r},\mathbf{r_m}\rangle/\lambda+\psi_0)}$. Here ψ_0 is some constant phase offset. The array output can then be written

$$E(t) = s(t)\sum_m w_m e^{2\pi i\langle \mathbf{r},\mathbf{r_m}\rangle/\lambda}$$

The static factor made by the sum in this expression is denoted the beam pattern for the array. The element locations $\mathbf{r_m}$ is fixed once and for all, but the filter weights $\{w_m\}_m$ can be selected to make the array antenna have high sensitivity in desired directions and suppress signals from other directions. AESA technology offers the possibility to change weights every frame, and DESA technology makes it possible for the computer to test many sets of filter weights every frame in order to produce an optimal result for the radar operator. Figure 1.1 is a schematic drawing of the time delay experienced by the antenna elements in a linear array for a monochromatic planar wave. In this case the time delay $\tau_m = -md\sin(\theta)/c$ where θ is the angle from boresight of the arriving wave.

1.2 Some beam patterns for linear array

The linear array is the array antenna of simplest geometry, and spatial filters for linear arrays are extensively studied, see e.g [4]. Spatial filters made by linear arrays are also used as building

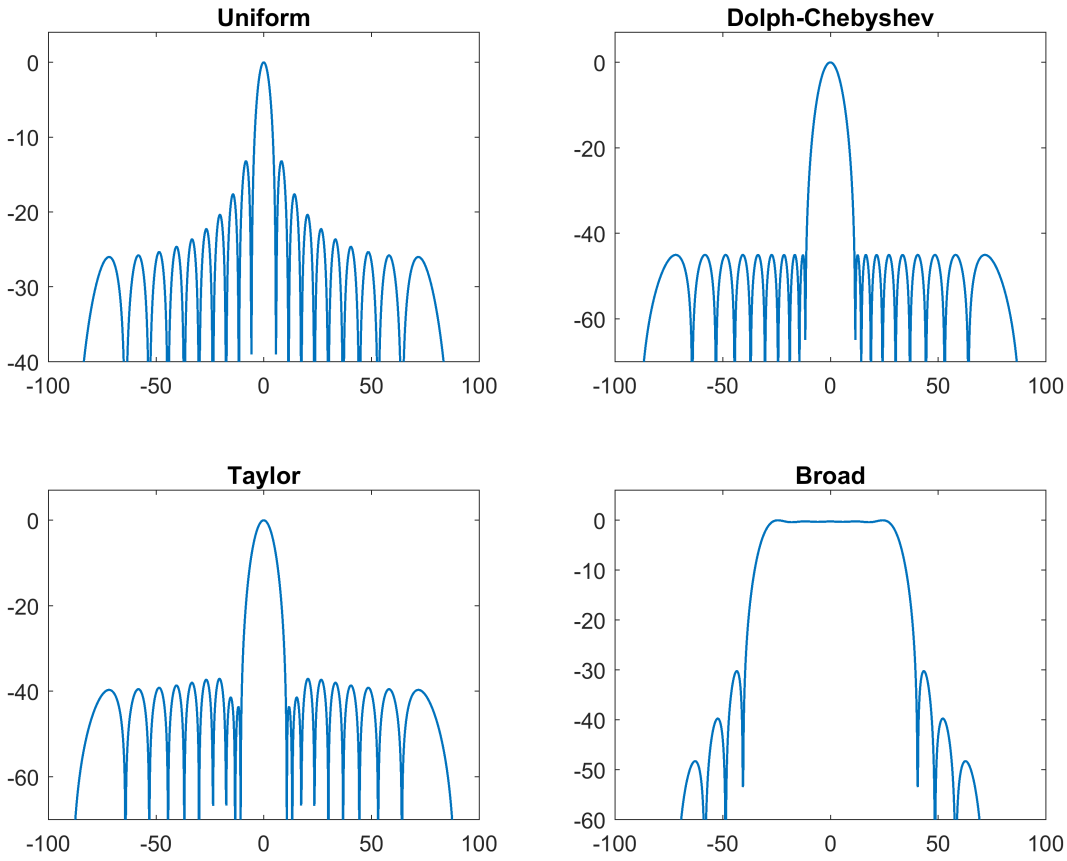

Figure 1.2 *Some beam patterns for linear array of 20 elements. Labels on horisontal axis indicate angle from boresight, and on vertical axis intensity in dB relative to the peak intensity*

blocks for more complex spatial filters. Many beam patterns for planar rectangular array antennas are achieved as products of beam patterns for linear arrays. In a linear array all the elements are located along the array axis and most commonly have a uniform spacing, d. When in addition the array elements are isotropic, the array output for a narrowband signal of wavelength λ is $E(t) = s(t) \sum_m w_m e^{2\pi i m \frac{d}{\lambda} \sin(\theta)}$. Figure 1.2 shows the static beam pattern for some choices of weights $\{w_m\}_m$. The intensity of the output from the spatial filter is plotted in logarithmic scale as a function of view angle. When all the element weights are equal, the resulting pattern is the periodic sinc function also denoted the uniform beam. Other patterns shown are examples of Dolph-Chebyshev and Taylor tapering for suppressing the sidelobes. Finally, a broad beam is synthesized by Woodwards method. The latter might be convenient in transmit mode when illuminating a wide area not very distant from the radar.

2 Acquisitions of synthetic target with Atlantis

2.1 Atlantis, test bed for digital beamforming

FFI has a passive coherent location (PCL) DESA system denoted Atlantis that can listen for and detect echoes of Digital Video Broadcasting - Terrestrial (DVB-T) signals. Illuminators of opportunity are television broadcasters. Atlantis is a research system developed by Fraunhofer FHR, and enhancements are continuously made to the system. Thirteen discone elements uniformly distributed along a linear array make the antenna. Due to coupling effects between neighbouring elements, only the eleven interior discone elements are actively receiving signals. The two outermost elements are placed there only to create a similar environment for secondmost outer elements as exists for the internal elements. Spacing between the elements is about 0.36m, and each discone element is oriented so as to have higher sensitivity for vertically polarized signals. The co-pol to cross-pol ratio is about 12dB for the discone element situated in the array. For each antenna element there is an AD-converter and the digitized signals from all the elements are processed in parallel by a computer system. The results after processing are presented on a console real time to the radar operator. The system can acquire signals within the frequency range 450-900MHz, and a selected center radio frequncy in this range is downconverted to intermediate frequency 76MHz before the signal is sampled at a rate of 64MHz. The digitized signals from each of the antenna elements are also stored in an archive and can be played back and be the subject of further experimentation. Processed data from the system like range-Doppler maps may also be archived. An acquisition experiment was conducted after an upgrade was made to the Atlantis system. During the experiement the DVB-T signal with center frequency 514MHz and bandwidth 8MHz was selected. For this DVB-T signal the ratio between element spacing and wavelength of carrier frequency is about 0.6. This ratio has an impact on the beam patterns generated, e.g at what angles greating lobes appear.

2.2 Experiment setup

The linear Atlantis array antenna was mounted horizontally on a lift and elevated about 5meters above ground. The lift with the antenna could be rotated. At a distance about 10km from the antenna the DVB-T transmitter in Bonn was located. The direction to the DVB-T transmitter was about $-14°$ from North as viewed from the Atlantis antenna. A synthetic target emulating a time delayed and Doppler shifted echo from the Bonn broadcaster was constructed by a repeater and transmitted from a log-periodic antenna located at the top of a nearby building. Doppler shift for the synthetic target was set at 81Hz and bistatic range 2.2km. The antenna transmitting the synthetic target signal was steadily located about $22°$ from North. A log-periodic antenna was used for this purpose, and the cross-polarization isolation for these kinds of antennas commonly lie in the range 20-25dB. At $8°$ from North about 10m from the Atlantis antenna there was another vertically polarized log periodic antenna transmitting an almost monochromatic tone. The monochromatic tone was used for real time calibration of the relative phase offsets of the antenna elements in the receiver array. Experiments for acquiring the synthetic target echo by the Atlantis system were made for various boresight directions of the Atlantis antenna relative to North. The global location

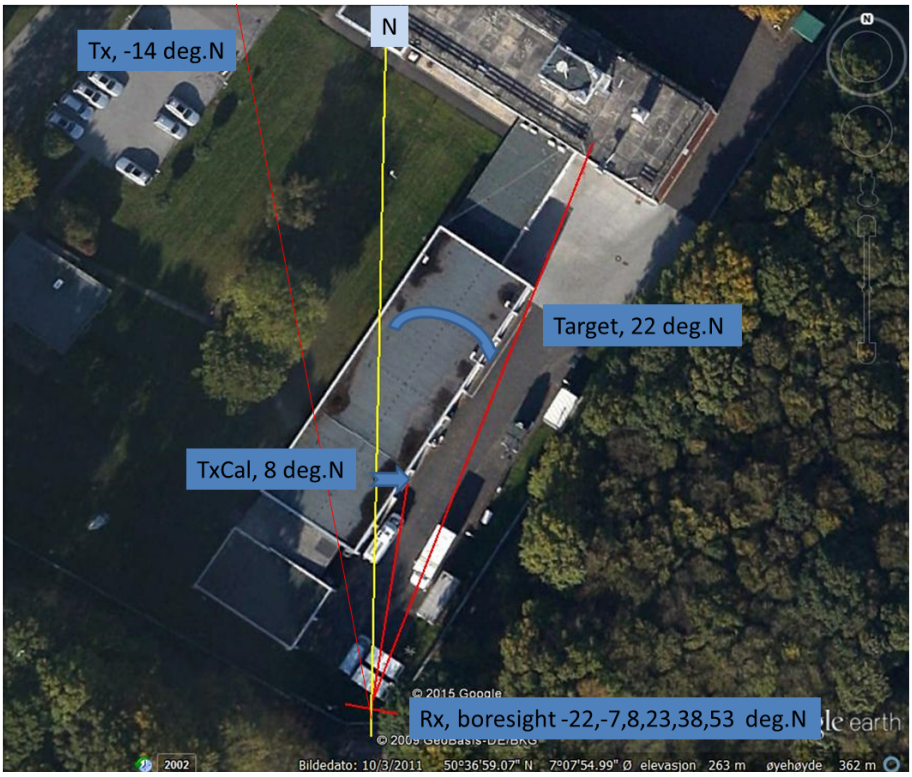

Figure 2.1 *Experiement configuration; Rx - Atlantis antenna, Tx - DVB-T transmitter, TxCal - calibration tone transmitter, Target - Transmitter synthetic target.*

of the antenna transmitting the synthetic target as well as the calibration antenna remained fixed during all acquisitions. Acquisitions were made for azimuth angle of the synthetic target equal to -31,-16,-1,14,29,44 degrees relative to antenna boresight. The corresponding azimuth angles to the calibration antenna were -45,-30,-15,0,15,30 degrees from boresight. Acquisitions for all the azimuth angles were repeated three times with various polarizations of the synthetic target echo transmitted by the log-periodic antenna. The polarizations were vertical, horizontal and diagonal. Figure 2.1 shows the location of the receiver antenna relative to the DVB-T transmitter as well as the calibration antenna and the synthetic target transmitter.

The acquisition experiment also served to compare the processing behavior for two Atlantis systems, that from the outset were supposed to behave the same. One of them beeing the FFI-system and the other one a system local to Fraunhofer FHR. The signal received by one and the same Atlantis antenna was split in two and sent to the two processing systems. The two systems processed the signal real time in parallell and presented the result on their respective operator consoles. The synthetic target appeared identical in the range-Doppler map (rD-map) consoles for both of the systems as well as in the plan position indicator consoles. According to these real time observations the systems behaved the same.

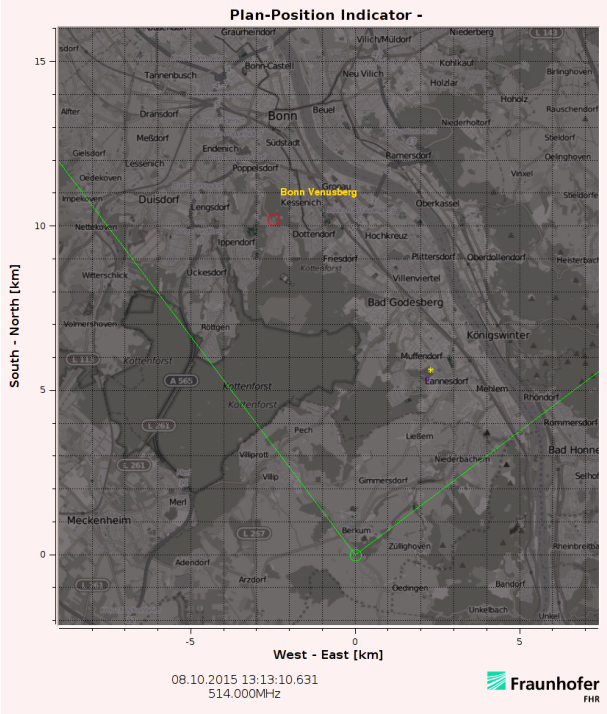

Figure 2.2 *Plan position indicator with target - yellow star, receiver antenna - green circle, and DVBT-transmitter - red circle. Asimuth angle determined by means of beamforming.*

2.3 Direction of arrival estimation

The plan position indicator in Figure 2.2 shows the detected target in a geographic coordinate map. To determine the longitude and latitude coordinates of the target, the azimuth of the target relative to the antenna boresight is needed in addition to the range. Mechanically rotating radars reveal the horisontal direction to the target as the target is highlighted when the mainlobe sweeps over target. The Atlantis antenna is not rotating mechanically, but by using digital beamforming techniques the system retrieves sufficient direction of arrival information from the target echo. For every data set acquired by the antenna and digitized, the computer processes the data set by many different spatial filters in parallel before a frame is finally presented on the radar operators console. The spatial filters consist of a set of beams obtained by scanning a chosen beam pattern in azimuth to a set of angles within the interval (-45°,+45°) from boresight. For every scan angle there is a beam and a corresonding rD-map is produced. For every beam all rD-cells with SNR above a given threshold are recorded together with their intensity level and azimuth of the mainlobe. The target detection associated with a particular rD-cell is then found to have direction from boresight given by the azimuth of the beam yielding the maximum intensity for the rD-cell.

3 DoA estimation based on rD-maps from Atlantis

The calculations leading up to Figure 2.2 were performed in real time by the Atlantis sofware processing the data acquired during the experiment at FHR. At the same time the recorded data was archived making it possible to process the data over again at a later stage using other methods. Data that had gone through some stages of the real time processing was also archived. For the remainder of this report we look at the archived data and process the data again by means of Matlab scripts.

In this section we take a closer look at the beamscan direction of arrival (DoA) estimation method. We perform beamscan with the uniform beam pattern as well as the Dolph-Chebyshev pattern. The Dolph-Chebyshev pattern is a classical tapering scheme for suppressing sidelobes, in the uniform beam pattern no tapering is applied. Both of the beam patterns are scanned by applying phase shifts to the output from each of the array elements.

Figure 3.1 shows the rD-map of a single antenna element to the left. The rD-map to the right is the one of an optimally scanned beam. The latter is formed by combining rD-maps for the single antenna elements as we now proceed to describe. An rD-map is a discrete approximation to the output of a matched filter comparing the input surveillance signal to time delays and Doppler shifts of a reference signal. We denote this bivariate function for the Doppler cross correlation function and use the symbol $\mathcal{X}(\tau, \nu)$,

$$\mathcal{X}(\tau, \nu) = \int s_{surv}(t)\overline{s}_{ref}(t-\tau)e^{-2\pi i\nu t}\,dt \tag{3.1}$$

Here the surveillance signal s_{surv} is the output from the array antenna after applicaton of the spatial filter. s_{ref} is the reference signal where the direct signal from the DVB-T transmitter constitutes the dominant part. We let $s^{\nu}_{surv}(t) = s_{surv}(t)e^{-2\pi i\nu t}$ denote the Doppler shifted surveillance signal. Changing the integration variable from t to $u = t - \tau$ in (3.1) we obtain $\mathcal{X}(\tau, \nu)$ as the cross correlation between the reference signal and the Doppler shifted surveillance signal, $\mathcal{X}(\tau, \nu) = s^{\nu}_{surv} \star s_{ref}(\tau)$. A match is obtained for given time delay and Doppler shift when $s_{surv}(t) = s_{ref}(t-\tau)e^{2\pi i\nu t}$. For every picture presented on the operator console in the Atlantis system, the computer calculates rD-maps for many beams. Since the cross-correlation product is linear in its first argument, we can easily calculate the rD-map for an arbitrary beam if we already have the rD-maps from each of the antenna elements. To see this, assume the surveillance signal beam is formed by scaling the output signals $\{s_m(t)\}_m$ by beam pattern coefficients $\{w_m\}_m$, so that $s_{surv}(t) = \sum_m w_m s_m(t)$. Using the notation $s^{\nu}_m(t) = s_m(t)e^{-2\pi i\nu t}$ for frequency shifted array element outputs, we may write

$$\mathcal{X}(\tau, \nu) = s^{\nu}_{surv} \star s_{ref}(\tau) = \sum_m w_m s^{\nu}_m \star s_{ref}(\tau) \equiv \sum_m w_m \mathcal{X}_m(\tau, \nu) \tag{3.2}$$

In a monostatic radar the reference signal is transmitted from the same location as the received signal, and the the matched filter (3.1) becomes a doppler shifted autocorrelation. In that case $\mathcal{X}(\tau, \nu)$ is denoted the range-Doppler ambiguity function. For more information on the range-Doppler ambiguity function see e.g [7].

The reference signal in (3.1) can be the output from an antenna with direct line of sight to the DVB-T transmitter. Many passive bistatic radar systems apply filters for supressing the direct

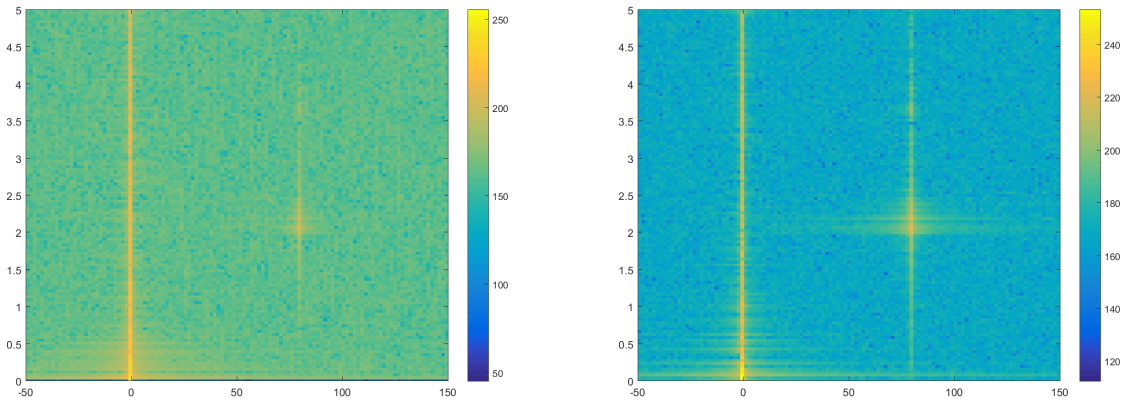

Figure 3.1 *Range-Doppler maps for single antenna element to the left and for an optimally scanned uniform beam to the right. Labels on horisontal axis indicate frequency in Hz and on vertical axis bistatic range in km. Colorbars indicate intensity in dB*

signal component in the surveillance signal. The Atlantis system however, performs a proper reconstruction of the DVB-T signal and uses that as the reference signal. The DVB-T signal is reconstructed by a method similar to the one described for DAB signals in [2]. In our acquisition experiment, the signal used for reconstruction of the DVB-T reference signal was acquired by the array antenna elements, no separate antenna was used for this purpose. During the acquisition experiment the Atlantis system calculated and archived range-Doppler maps for each of the antenna elements, i.e discretisations of $\{\mathcal{X}_m(\tau, \nu)\}_m$ in (3.2). These elementwise rD-maps are used when producing the SNR-plots presented in the remainder of this report.

3.1 Tests with Uniform pattern

Looking at the rD-map for a single antenna element in figure 3.1 we find that the rD-map has a local maximum for the intensity at the cell with bistatic range 2.2km and Doppler 81Hz. For the same data set as was used to produce figure 3.1 we have calculated rD-maps for more than 100 scanned beams, using uniform weights $\{w_m\}_m$. The scan angle is running from -90°to +90°. The rD-maps for all the beams are formed by taking linear combinations of the rD-maps for each of the antenna elements, like in (3.2). For every scan angle the corresponding scanned beam produces an rD-map. In each of these rD-maps we have read off the signal value at the very same range and Doppler location. The location is given by the target-signal peak in the single channel rD-map produced by any one of the antenna array elements, and is found at rD-location (2.2km, 81Hz). The noise level entering the signal to noise ratio (SNR) for each of the scanned beams is taken as the root mean square intensity value in the two far rD-quadrants of the corresponding rD-map. Figure 3.2 shows the SNR of the rD-cell as a function of the beam scan angle. As can be seen from the rightmost figure, a peak is observed at 14 degrees from boresight. This acquisition was made for antenna boresight pointing 8 degress North. The peak at 14 degrees off boresight therefore corresponds well to the actual location of the antenna transmitting the synthetic target, see figure 2.1.The leftmost plot in figure 3.2 shows similar signal peak location for data set acquired with antenna boresight

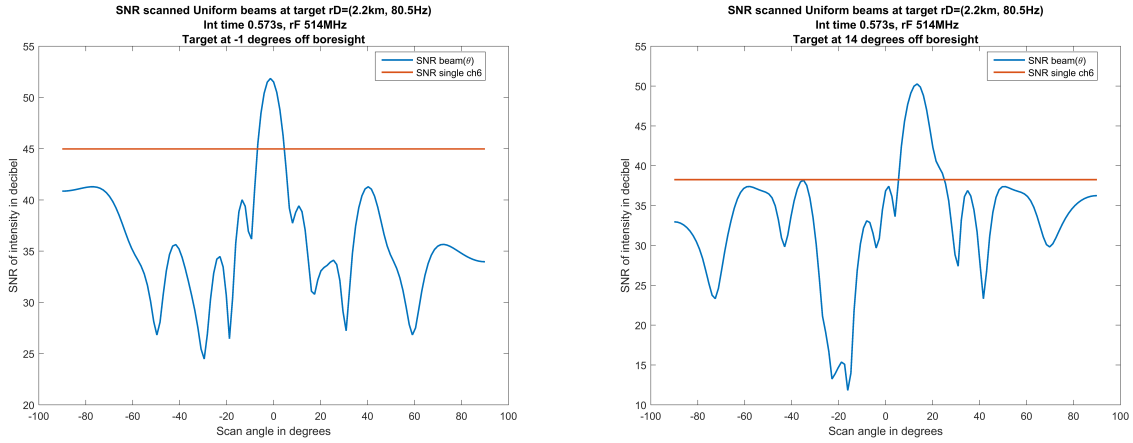

Figure 3.2 *SNR as function of scan angle for fixed range-Doppler cell of synthetic target, range 2.2km Doppler 81Hz, and uniform beam pattern. Location of synthetic target at* -1° *from boresight for left plot and at* 14° *for right plot.*

at 23°North, corresponding to target arriving -1degree from boresight. For comparison purposes the figures also contain the SNR for the omnidirectional beam of the single element located at the array center. The array antenna obtained an improvement in peak SNR of 8-13 dB compared to the omnidirectional beam of a single array element. The SNR for the other single array elements where also calculated and showed some mutual variation up to 5 dB (not shown here). The gain in SNR for the array compared to the single elements is in accordance with the theory for uniform linear arrays of omnidirectional elements. When the element spacing is half the wavelength and the weights uniform, the SNR is proportional to the number of elements for narrowbanded signals and noise identically distributed and uncorrellated between the elements, [9]. Similar measurements were made for all the six antenna directions 53,38,23,8,-7,-22 degrees relative to north. They show similar results, as can be seen in figures 3.4 and 3.6 in the next section.These antenna directions correspond to target signal arriving -31,-16,-1,14,29,44 degrees in azimuth from boresight.

When considering these plots it can be useful to have a rough idea of when to expect greating lobes. An estimate can be obtained by considering the beam pattern for omnidirectional array elements and uniform weights. In that case the beam pattern is the Dirichlet kernel, also called the periodic sinc function. For scan angle θ_0 greating lobes appear at θ satisfying $\sin\theta - \sin\theta_0 = j\lambda/d$ where $j \in \mathbb{Z}$, and d is the element spacing. In our experiment setup $d/\lambda = 0.6$, and for this ratio the first greating lobe for the periodic sinc function appears when scanning the beam to about $\arcsin \pm(1 - 1/0.6) = \pm 48^\circ$.

3.2 Tests with Dolph-Chebyshev pattern

We also calculated the SNR ratio for the target-cell at bistatic range 2.2km and Doppler 81Hz when all the scanned beams had the Dolph-Chebyshev pattern. We can see from the plot 3.3 that the mainlobe broadenes a bit and that the SNR ratio was reduced to some extent. The Dolph Chebyshev pattern used for this application has sidelobe level -55dB relative to the main lobe. Comparing these SNR plots with those for the uniform beam pattern we would have expected a greater reduction in

the side lobe level.

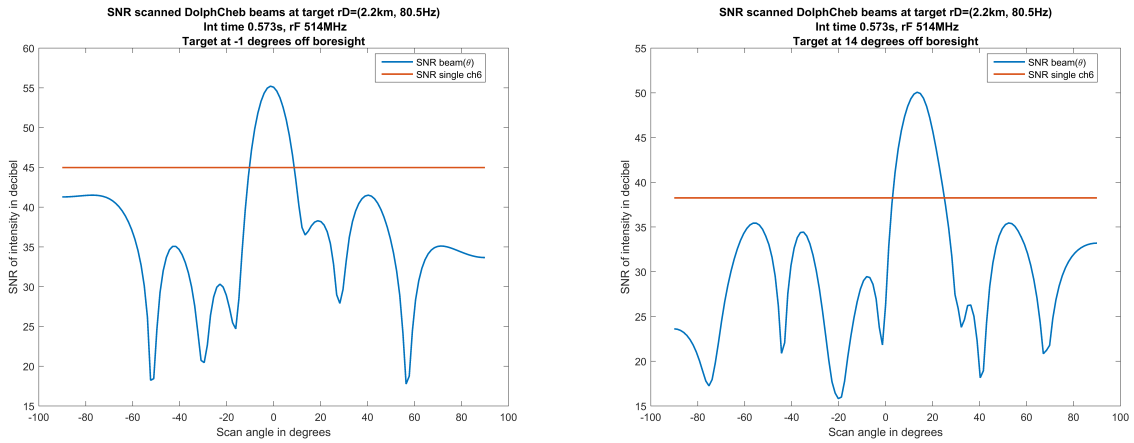

Figure 3.3 *SNR as function of scan angle for fixed range-Doppler cell of synthetic target, range 2.2km Doppler 81Hz, and Dolph-Chebyshev pattern. Location of synthetic target at* -1° *from boresight for left plot and at* 14° *for right plot.*

3.3 Cross-polarized target signal

The figures in the previous sections show acquired signals where the synthetic target was transmitted from a vertically polarized log-periodic antenna. The transmitted target signal during that part of the acquisition experiment was therefore mainly co-polarized with the vertically polarized Atlantis receiver antenna. Even though the discone elements of the Atlantis antenna are vertically polarized they do not isolate completely for horisontally polarized signals. It is therefore of interest to study the behavior of the antenna for signals that are horisontally-polarized as well as for signals that contain a substantial horisontal component in addition to a vertical component. The acquisition experiment was conducted for these polarizations of the synthetic target signals.

In the first case the transmitter antenna from the first part of the experiment was simply rotated 90 degrees, so that the main component of the target signal was cross-polarized with the receiver antenna. SNR calculations similar to those in the previous sections were performed for the acquisition of the horisontally polarized target signal. The synthetic target emulated by the DVB-T signal repeater was transmitted with the same time delay and Doppler shift as for the co-polarized case. Figures 3.4, 3.6 show the SNR plots for these acquisitions when the synthetic target transmitter antenna is located at 6 different angles between -31°and 44°off boresight. In the same figures we have also included the SNR for the vertically polarized target transmitter antenna as well as the diagonally polarized target signal. The diagonally polarized signal was transmitted with the log periodic antenna rotated about 45°from the vertical line. The plots clearly show a much lower SNR ratio for the target peak of the horizontally polarized signal compared to the vertically polarized one, about 15dB. The low gain for the cross-polarized signal should be expected, more interesting is perhaps the displacement of the SNR-peak for the horisontally polarized signal relative to the vertically polarized signal observed for some of the azimuth locations of the transmitted target signal. The displacement is about 20°for the case where the transmitted signal is boresight to

the receiver antenna. These varying peak locations indicate that the array antenna diagram for horisontally polarized signal is dependent on the azimuth angle. One can therefore expect some difficulty in direction of arrival estimation for signals that are mainly cross-polarized with the array antenna elements.

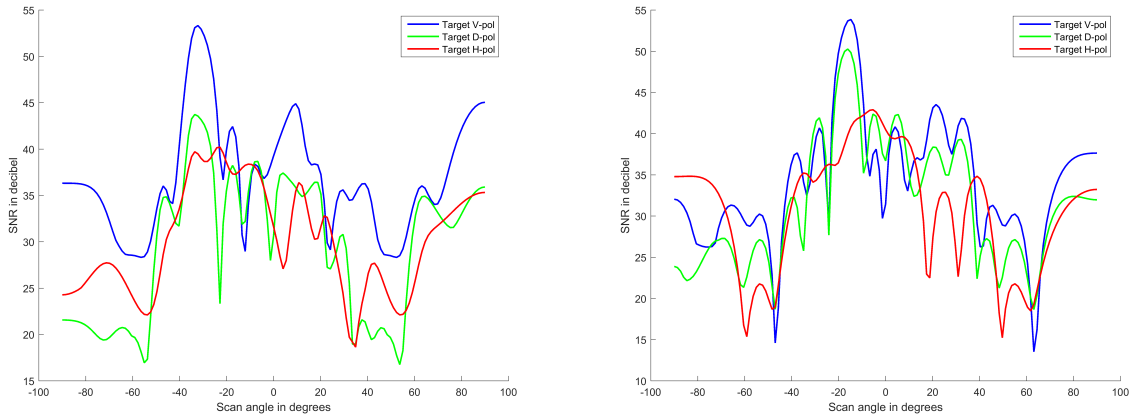

Target at $-31°$ (left) and $-16°$ (right) from boresight

Figure 3.4 *SNR as function of beam scan angle for fixed range-Doppler cell of target, range 2.2km Doppler 81Hz. Uniform beam pattern. Synthetic target signal polarisation Vertical (blue), Horisontal(red) and Diagonal(green).*

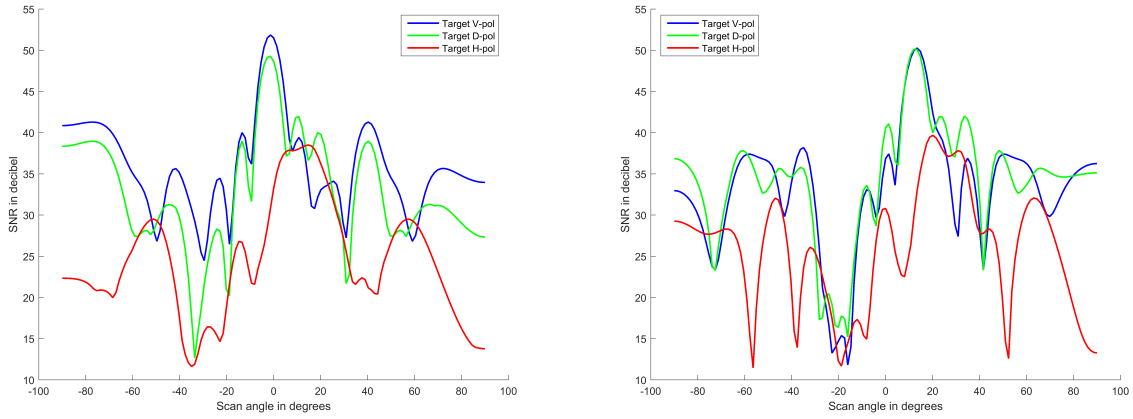

Figure 3.5 *Target at $-1°$ (left) and $14°$ (right) from boresight*

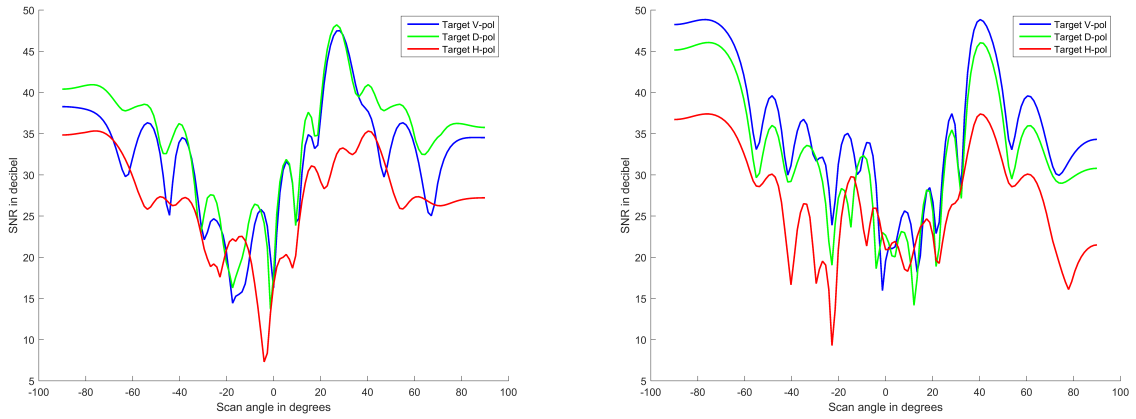

Figure 3.6 *Target at* $29°$ *(left) and* $44°$ *(right) from boresight*

We processed the data sets from vertically, horisontally and diagonally polarized signals over again using the Dolph-Chebyshev beam pattern. Like before the sidelobe ratio for the pattern was 55dB. Similar trends for the SNR at the target rD-cell show up as for the uniform case. In figure 3.7 we can see a notable displacement of the mainlobe for the horisontally polarized signal. Plots for target signal transmitted at -16,-1,14,29 degrees from boresight are shown. The Dolph-Chebyshev beam pattern with sidelobe ratio 55dB has a relatively wide mainlobe compared to the one for the uniform beam. This is reflected in the SNR-plots. The curves for the Dolph-Chebyshev pattern are smoother than those for the uniform pattern.

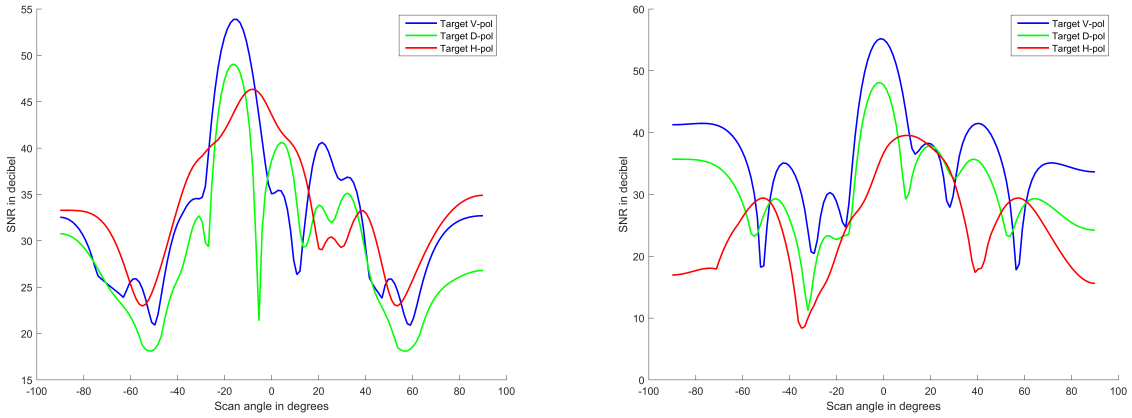

Target at $-16°$ *(left) and* $-1°$ *(right) from boresight*

Figure 3.7 *SNR for target signal in rD-map as function of beam scan angle, Dolph-Chebyshev beam pattern. Target signal polarisation Vertical (blue), Horisontal(red) and Diagonal(green).*

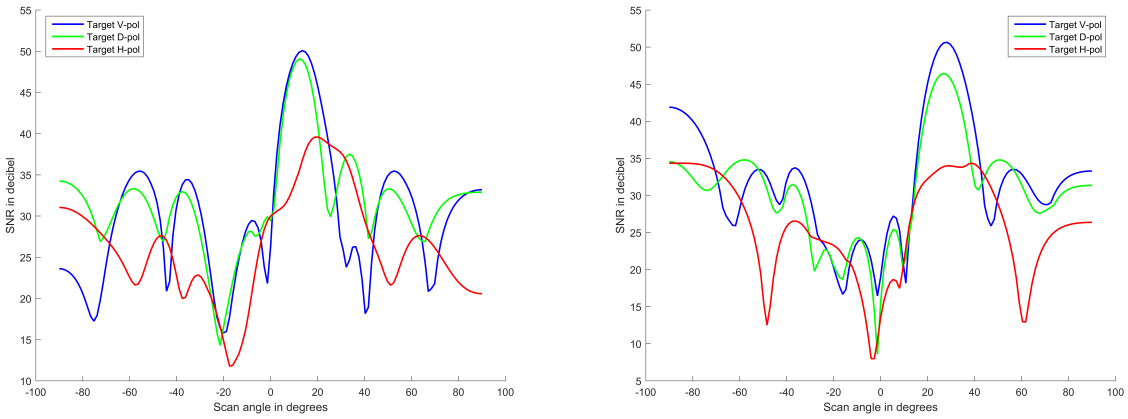

Figure 3.8 *SNR target signal as function of scan angle. Target at* $14°$ *(left) and* $29°$ *(right) from boresight, otherwise same as figure 3.7*

4 Placing a null at the target direction

A common technique for reducing jammer interference is to use a beam pattern that suppresses signals arriving from the direction of the jammer. In this section we consider the synthetic target located about 22°from North relative to the Atlantis antenna to be the signal we want to supress. There are two parts to this problem. First the direction of arrival has to be determined, and secondly a null should be placed in that direction. Here we consider only the second part. Since we know the direction of arrival, we can test the effect of a particular scheme for placing a null at a specified direction. The scheme for calculating the coefficients of the spatial filter is a quadratic optimisation problem that strives for preserving a given beam pattern while simultaneously placing a null at a specified direction. The figures in this section show signal acquired during a session where the synthetic target was transmitted from an antenna with vertical polarization. We should emphesize that in figures 4.3-4.5 the nulling direction and the target signal direction is the very same. One might expect that nulling the target signal direction would cancel the signal totally. As we will see this is not the case. However, a substantial reduction is achieved.

In the following we give some details on the scheme used for placing nulls in an existing beam pattern. Let the column vector $\mathbf{B}(\theta)$ be the elementwise E-field pattern in direction θ of a linear array of N isotropic elements

$$\mathbf{B}(\theta) = \{e^{2\pi i n \frac{d}{\lambda}\sin\theta}\}_n\,,\ n = -(N-1)/2, ..., (N-1)/2$$

For a desired scan direction θ_d we write $\mathbf{B_d} = \mathbf{B}(\theta_d)$. Assume we are given beam pattern coefficients $\mathbf{a} = \{a_n\}_n$ with corresponding diagonal matrix $\mathbf{A} = \mathrm{diag}(\mathbf{a})$. We want to find new beam pattern coefficients $\mathbf{w} = \{w_n\}_n$ such that

$$\begin{aligned} &\max_{\|\mathbf{w}\|=1} \mathbf{w^h A^t \overline{B}_d B_d^t \overline{A} w} \\ &\text{subject to } \mathbf{Gw} = \mathbf{0} \quad \text{where} \\ &\qquad \mathrm{row}_j\mathbf{G} = \mathbf{B^t}(\theta_j) \end{aligned} \tag{4.1}$$

The norm $\|\cdot\| = \|\cdot\|_2$ is the 2-norm in $\mathbb{C}^N$, also denoted the euclidean norm. The notation $\mathbf{w^h}$, $\mathbf{w^t}$ and $\overline{\mathbf{w}}$ is used for the Hermitian, transpose and conjugate of $\mathbf{w}$. When there are no constraints, the optimal coefficients are $\tilde{\mathbf{a}} = \mathbf{A}\overline{\mathbf{B}}_\mathbf{d}$ corresponding to scanning the beam the desired direction. An optimal solution to the constrained problem is obtained by projecting the solution for the unconstrained problem onto Null($\mathbf{G}$), the null space of $\mathbf{G}$. By means of the pseudo inverse $\mathbf{G}^+$ of $\mathbf{G}$ we can construct the linear map $\mathbf{I} - \mathbf{G}^+\mathbf{G}$ that is an orthogonal projector onto Null($\mathbf{G}$), see e.g [1]. This projector provides the solution to (4.1)

$$\mathbf{w} = \frac{\tilde{\mathbf{a}}_\parallel}{\|\tilde{\mathbf{a}}_\parallel\|} \quad \text{where } \tilde{\mathbf{a}}_\parallel = (\mathbf{I} - \mathbf{G}^+\mathbf{G})\tilde{\mathbf{a}} \text{ and } \tilde{\mathbf{a}} = \mathbf{A}\overline{\mathbf{B}}_\mathbf{d} \tag{4.2}$$

An outline of the setup (4.1) with solution (4.2) is given for the uniform case in [5] p.104. For completeness we include an argument here for general beam pattern coefficients $\mathbf{a}$. First, note that for any $\mathbf{v} \in \mathrm{Null}(\mathbf{G})$ we have $\langle \mathbf{v}, \tilde{\mathbf{a}}\rangle = \langle \mathbf{v}, \tilde{\mathbf{a}}_\parallel\rangle$. Moreover, $\langle \tilde{\mathbf{a}}_\parallel, \tilde{\mathbf{a}}\rangle = \|\tilde{\mathbf{a}}_\parallel\|^\mathbf{2}$. Using this in the optimisation problem (4.1), we get $\mathbf{v^h\tilde{a}\tilde{a}^h v}/\|\mathbf{v}\|^\mathbf{2} = \langle \mathbf{v}/\|\mathbf{v}\|, \tilde{\mathbf{a}}_\parallel\rangle^\mathbf{2} \le \langle \tilde{\mathbf{a}}_\parallel/\|\tilde{\mathbf{a}}_\parallel\|, \tilde{\mathbf{a}}_\parallel\rangle^\mathbf{2} = \tilde{\mathbf{a}}_\parallel^\mathbf{h}\tilde{\mathbf{a}}\tilde{\mathbf{a}}^\mathbf{h}\tilde{\mathbf{a}}_\parallel/\|\tilde{\mathbf{a}}_\parallel\|^\mathbf{2}$. The inequality in this expression is strict unless $\mathbf{v}$ is parallel to $\tilde{\mathbf{a}}_\parallel$. Hence (4.1) has a unique solution as long as $\tilde{\mathbf{a}}_\parallel \neq \mathbf{0}$, or equivalently as long as $\tilde{\mathbf{a}}$ does not lie in the range of $\mathbf{G^h}$.

Figure 4.1 shows the theoretical monochomatic beam pattern for the uniform beam and the Dolph-Chebyshev beam modified by inserting a null in the sidelobe as described by (4.2). Except for the location of the null, the beam pattern is not very different from the original pattern. Like in the Atlantis antenna, there are 11 elements in the array. Three close nulls 0.5° apart are placed in the sidelobe as well as in the main lobe of the uniform beam in figure 4.2. Three close nulls in the sidelobe make a greater difference to the original pattern than a single null, the split is broader and the sidelobe level goes up. When inserted into the main lobe, the main lobe is split and there is a substantial raise in the sidelobe level, although the beam still has some directivity.

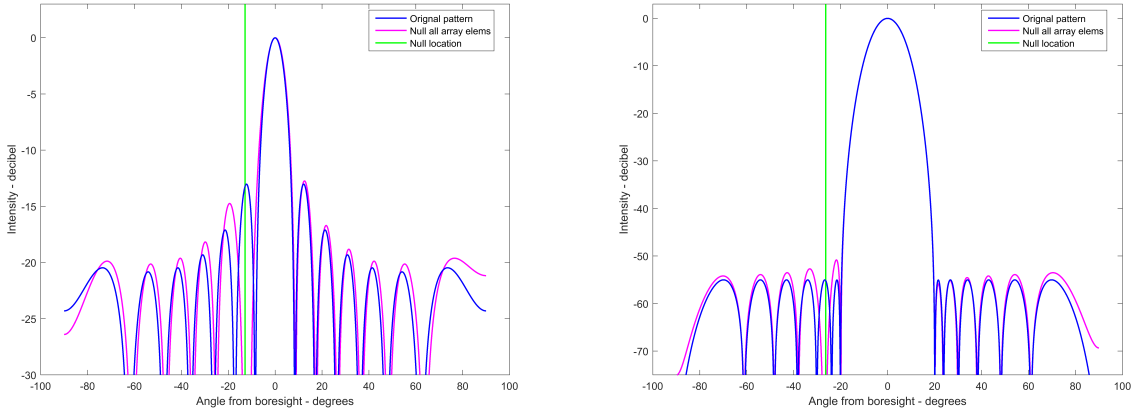

Figure 4.1 *Uniform(left) and Dolph-Chebyshev(right) patterns with single null in sidelobe, original pattern -blue, and null-modified -magenta*

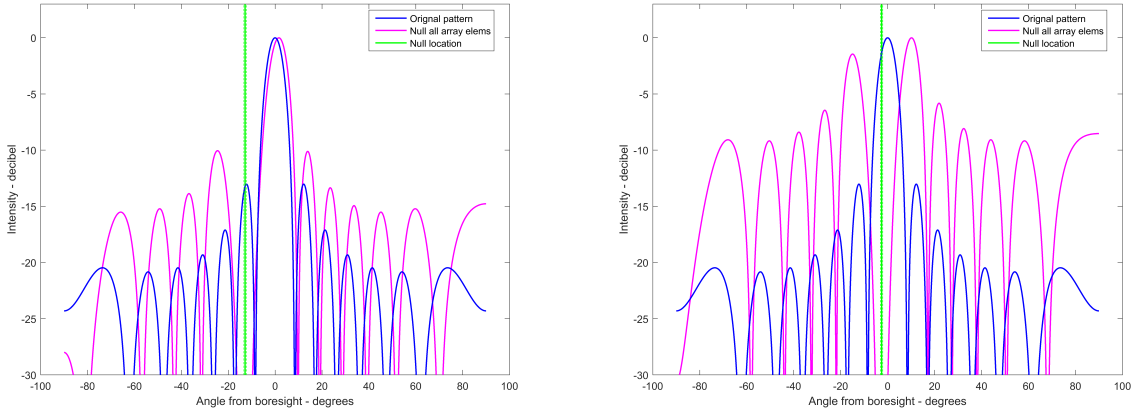

Figure 4.2 *Uniform pattern(blue) with 3 close nulls(magenta). Left plot shows nulls in sidelobe, and right plot nulls in main lobe*

Using the nulling methods of (4.1) we tried to suppress the signal from the synthetic target in the data acquired during the experiment described in section 2. Like in the previous section we calculated the range doppler map for the null-modification of the uniform beam at a number of scanned angles in the interval (-90°,90°) while reading off the SNR at the rD-cell corresponding to

the location of the synthetic target. For each of the scan angles the uniform pattern was modified by a null placed in the direction of the synthetic target. As the main lobe swept across the angle interval, the null travelled through all the sidelobes as well as the main lobe of the uniform beam. Figures 4.3 and 4.4 show the SNR for the rd-cell of the synthetic target location. The red dotted curve shows the SNR for the uniform beam pattern with a single null placed in the direction of the target, and for the red solid curve there are three nulls placed in the direction of the target. The three nulls are separated by half a degree. The blue line shows the SNR for the original uniform beam pattern with no nulls. The vertical green line indicate the location of the synthetic target which also coincides with the null location. The peak SNR is reduced by approximately 10dB for the beam pattern with a single null. Inserting three closely seprated nulls in the beam pattern makes a substially broader null, and the SNR is also seen to be much lower when the nulled target location is within $\pm 20^\circ$ from the main lobe. When the nulled target location appears in the side lobes further away from main lobe, the nulling has no effect. In the latter case the SNR at the nulled target location is just as strong as for the case where no nulling was done. No proper zero appears in any of the plots. The DVB-T signal has bandwidth about 2% of the carrier frequency. Consequently the null for the center frequency will be shifted notably for the frequency at the border of the band. This could partly explain why no proper null is seen in the plot.

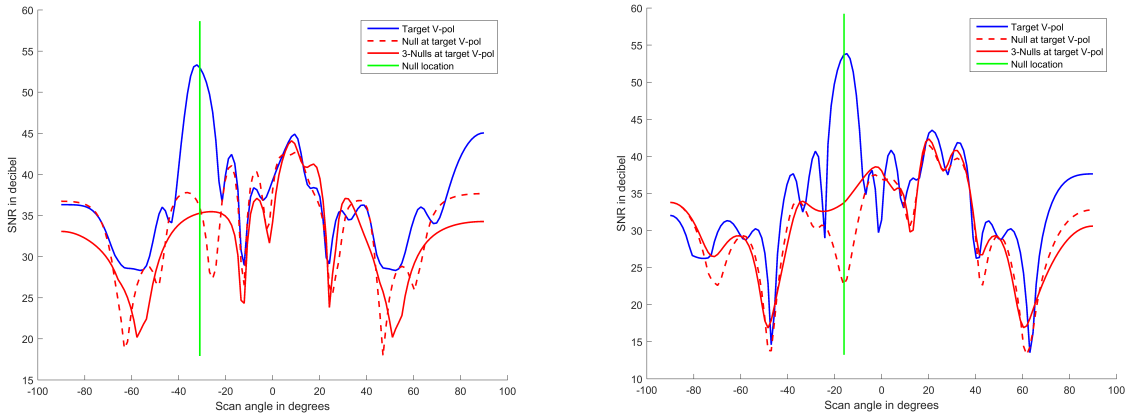

Target and null at -31° (left) and -16° (right) from boresight

Figure 4.3 *SNR as function of beam scan angle for fixed range-Doppler cell of target, range 2.2km Doppler 81Hz. Uniform beam with single null (dotted red line) and three close nulls (solid red line) placed at target direction. Uniform beam without null (blue line)*

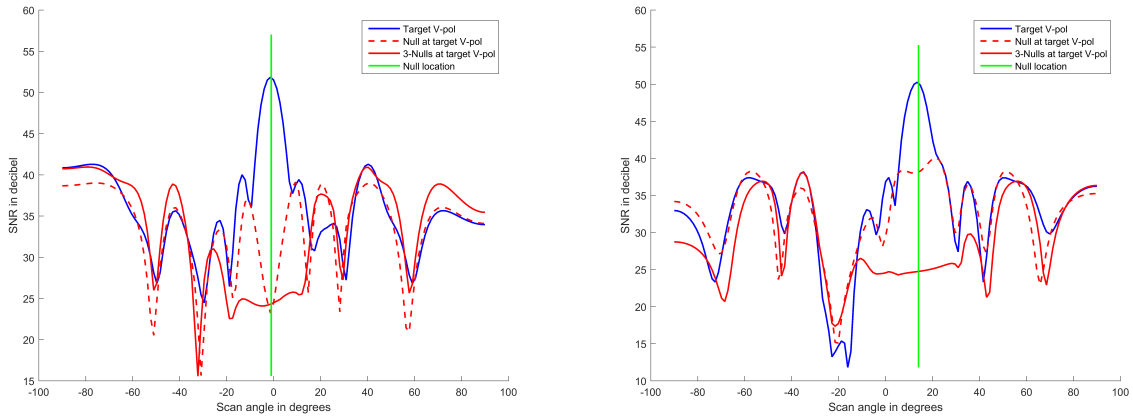

Target and null at $-1°$ (left) and $14°$ (right) from boresight

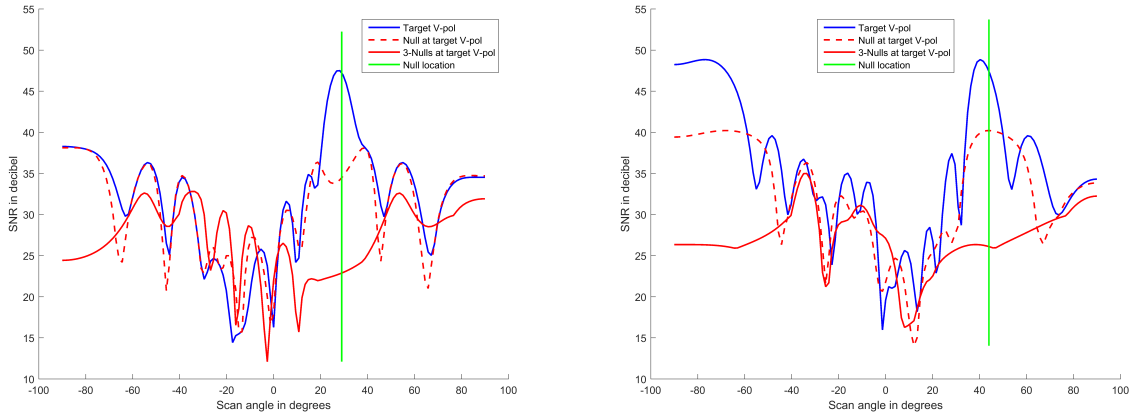

Target and null at $29°$ (left) and $44°$ (right) from boresight

Figure 4.4 *SNR for rD-cell of target as function of scan angle. Same as figure 4.3 except for other nulled target directions*

Similar behavior is seen for the Dolph-Chebyshev pattern. Inserting three close nulls lowers the SNR substantially in a neighbourhood of the main lobe, and inserting a single null mainly has an effect in a narrower region near the main lobe, figure 4.5.

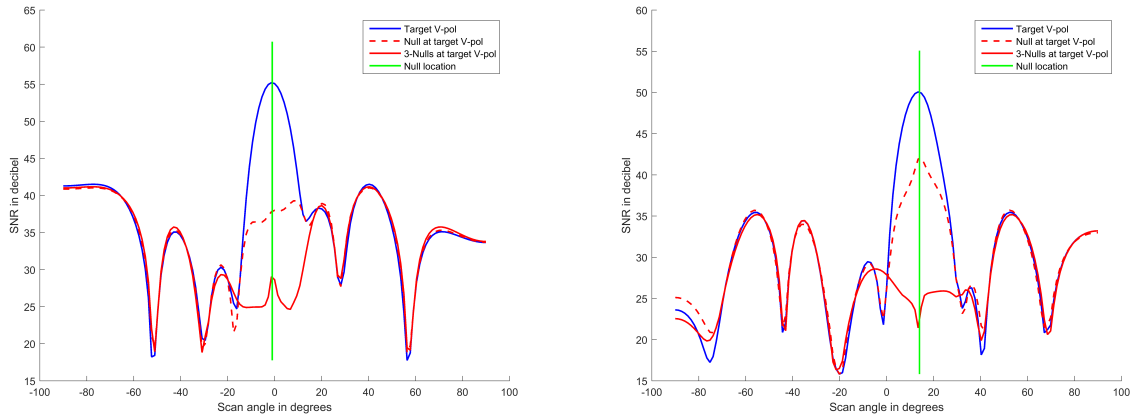

Target and null at $-1°$ (left) and $14°$ (right) from boresight

Figure 4.5 *SNR as function of beam scan angle for fixed range-Doppler cell of target, range 2.2km Doppler 81Hz. Dolph-Chebyshev beam with single null (dotted red line) and three close nulls (solid red line) placed at target direction. Dolph-Chebyshev beam without null (blue line)*

Since the DVB-T signal in Atlantis has a substantial bandwidth, one might suspect that inserting nulls in the sidelobe could have a greater effect on the mainlobe than what is the case for the theoretical monochromatic beam pattern of figures 4.1,4.2. This is however not the case. For example, placing a null in the direction of the DVB-T transmitter that is located $22°$ from the synthetic target, has no substantial effect on the SNR at the rD-cell of the synthetic target. We do not include any such plots since they are more or less equal to the SNR -plot for the target rD-cell when no nulls are inserted into the beam.

4.1 Nulling of cross-polarized signal

It was seen above that DoA estimation was problematic for signals cross-polarized with the discone antenna elements of the Atlantis system. When however there was a substational co-polarized component in the target signal, DoA estimation worked fairly well. Similar behavior can be seen for the beam patterns placing a null in the direction of the target. Nulling a totally cross-polarized signal does not work. Placing a single null in the direction of a diagonally polarized target signal works somewhat better. This is done for the uniform beam pattern in figure 4.6

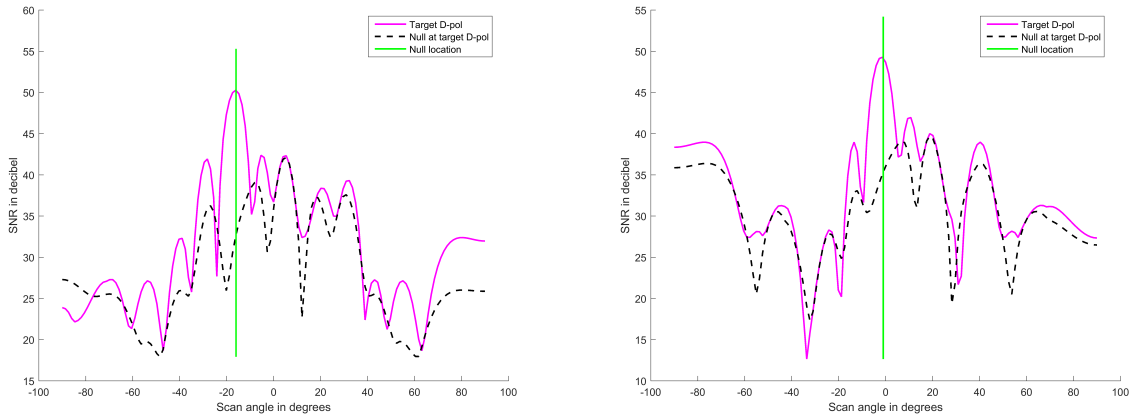

Target and null at $-16°$ (left) and $-1°$ (right) from boresight

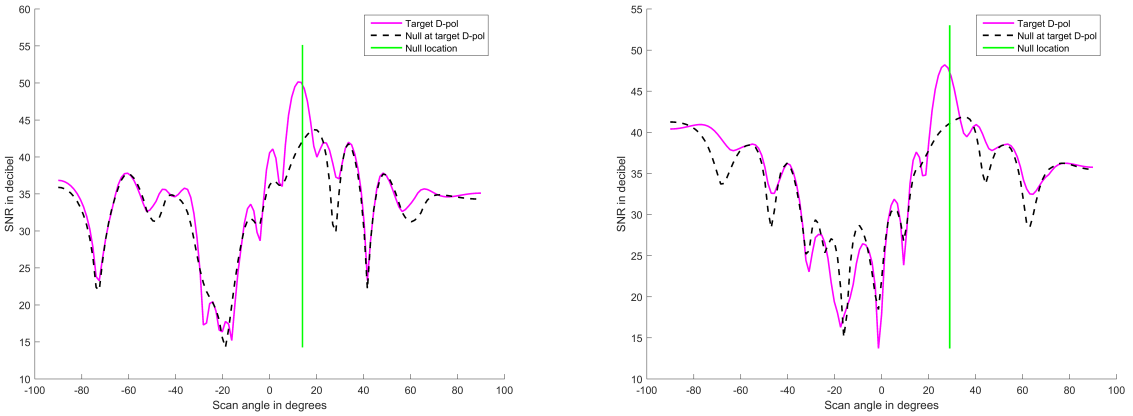

Target and null at $14°$ (left) and $29°$ (right) from boresight

Figure 4.6 *SNR diagonally polarized signal at target rD-cell. Uniform beam(magenta), Uniform with single null at target (black dotted)*

5 Conclusion

Narrowband beamforming techniques for DoA estimation and nulling have been recalled briefly and applied to a real data set. The data set is acquired by a passive radar with a linear array antenna of 11 discone elements. The acquisitions were made with a synthetic target radar echo, allowing for adjustment of the echo polarization.

DoA estimation by beamscan worked successfully for target echoes that were co-polarized with the array antenna polarization. The array antenna obtained an improvement in peak SNR of about 10 dB compared to the omnidirectional beam of a single array element. This compares well to the theoretical SNR for a uniform linear array of omnidirectional elements. We observed somewhat higher peak to sidelobe ratio for the SNR of the Dolph-Chebyshev pattern than for the uniform beam pattern, but the peak location was sharper for the uniform beam. Severe problems appeared for signals cross-polarized with the array antenna. A substantial decrease in SNR was observed, as well as an artificial shift in azimuth for the peak SNR location. For signals with co- and cross-polarized components of approximately the same size DoA estimation worked well even though the SNR was somewhat lower than for purely co-polarized signals.

A quadratic problem with equality constraints was used for calculating array element weights placing nulls in a given beam pattern. Both the Dolph-Chebyshev pattern and the uniform beam pattern were tested. One or three static nulls were placed in the direction of the synthetic target. Significant suppresion of the signal was demonstrated for azimuth angles within 20°of the main lobe direction. Three close nulls located about 1°apart caused a broader suppression in azimuth than was achieved by a single null. These observations on nulling were made for signals co-polarized with the array antenna. Like for DoA estimation the nulling had severe problems with purely cross-polarized signals.

Acknowledgement

The Atlantis PCL system is constructed at Fraunhofer FHR, and we are indebted to the researchers that have participated in developing the system. We would like to thank Jörg Heckenback and Diego Cristalline at Fraunhofer FHR for organizing the acquisition experiment underlying this report.

Bibliography

[1] G.H.Golub, C.F.Van Loan *Matrix Computations 3rd edition* Johns Hopkins University Press, 1996, ISBN 978-0-8018-5414-9

[2] D.W.O'Hagan, H.Kuschel, J.Heckenback, M.Ummenhofer and J.Schell *Signal Reconstruction as an Effective Means of Detecting Targets in a DAB-based PBR*, Radar Symposium (IRS), 11th International, 2010, ISBN 978-1-4244-5613-0

[3] D.H.Johnson, D.E.Dudgeon *Array Signal Processing: Concepts and Techniques*, Prentice Hall, Englewood NJ, 1993

[4] R.J.Mailloux *Phased Array Antenna Handbook, 2nd edition*, Artech House, Inc. 2005, ISBN 1-58053-689-1

[5] W.L. Melvin and J.A. Scheer (eds) *Principles of Modern radar, Advanced Techniques*, SciTech Publishing 2013, ISBN 978-1-891121-53-1

[6] R.A.Monzingo, R.L.Haupt, T.W.Miller *Introduction to Adaptive Array, 2nd edition*, SciTech Publishinc 2011, ISBN 978-1-891121-57-9

[7] M.A.Richards, J.A.Scheer, W.A.Holm (eds) *Principles of Modern radar, Basic Principles*, SciTech Publishing 2010, ISBN-13 978-9746522-00-7

[8] G.W. Stimson, H.D. Griffiths, C.J. Baker, D. Adamy *Stimsons's Introduction to Airborne Radar, 3rd edition*, SciTech Publishing, 2014, ISBN 978-1-61353-022-1.

[9] H.L.Van Trees *Optimum Array Processing, Part IV of Detection, Estimation and Modulation Theory*, Wiley India Pvt.Ltd, 2013, ISBN 978-81-265-3847-8.

About FFI

The Norwegian Defence Research Establishment (FFI) was founded 11th of April 1946. It is organised as an administrative agency subordinate to the Ministry of Defence.

FFI's MISSION

FFI is the prime institution responsible for defence related research in Norway. Its principal mission is to carry out research and development to meet the requirements of the Armed Forces. FFI has the role of chief adviser to the political and military leadership. In particular, the institute shall focus on aspects of the development in science and technology that can influence our security policy or defence planning.

FFI's VISION

FFI turns knowledge and ideas into an efficient defence.

FFI's CHARACTERISTICS

Creative, daring, broad-minded and responsible.

Om FFI

Forsvarets forskningsinstitutt ble etablert 11. april 1946. Instituttet er organisert som et forvaltningsorgan med særskilte fullmakter underlagt Forsvarsdepartementet.

FFIs FORMÅL

Forsvarets forskningsinstitutt er Forsvarets sentrale forskningsinstitusjon og har som formål å drive forskning og utvikling for Forsvarets behov. Videre er FFI rådgiver overfor Forsvarets strategiske ledelse. Spesielt skal instituttet følge opp trekk ved vitenskapelig og militærteknisk utvikling som kan påvirke forutsetningene for sikkerhetspolitikken eller forsvarsplanleggingen.

FFIs VISJON

FFI gjør kunnskap og ideer til et effektivt forsvar.

FFIs VERDIER

Skapende, drivende, vidsynt og ansvarlig.

FFI's organisation

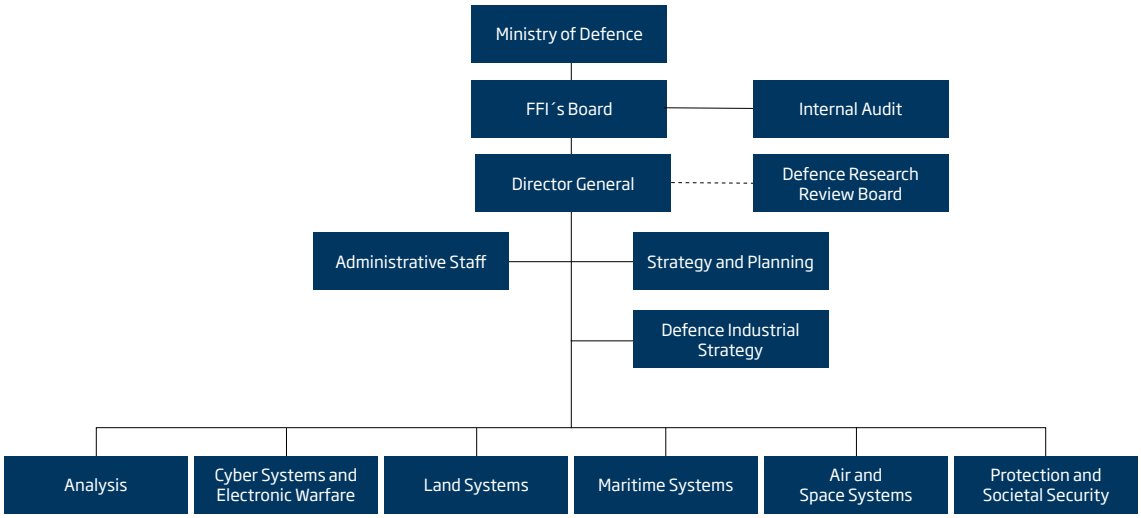

Forsvarets forskningsinstitutt
Postboks 25
2027 Kjeller

Besøksadresse:
Instituttveien 20
2007 Kjeller

Telefon: 63 80 70 00
Telefaks: 63 80 71 15
Epost: ffi@ffi.no

Norwegian Defence Research Establishment (FFI)
P.O. Box 25
NO-2027 Kjeller

Office address:
Instituttveien 20
N-2007 Kjeller

Telephone: +47 63 80 70 00
Telefax: +47 63 80 71 15
Email: ffi@ffi.no

FFI Forsvarets forskningsinstitutt
Norwegian Defence Research Establishment